

Strong paramagnon scattering in single atom Pd contacts

V. Schendel,^{1,*} C. Barreteau,^{2,3} M. Brandbyge,³ B. Borca,¹ I. Pentegov,¹ U. Schlickum,¹ M. Ternes,¹ P. Wahl,^{4,1} and K. Kern^{1,5}

¹Max-Planck-Institut für Festkörperforschung, Heisenbergstraße 1, 70569 Stuttgart, Germany

²Service de Physique de L'Etat Condensé (SPEC), CEA, CNRS,

Université Paris-Saclay, CEA Saclay 91191 Gif-sur-Yvette Cedex, France

³Dept. of Micro and Nanotechnology, Tech. Univ. of Denmark, Ørsteds Plads build. 345B, DK-2800 Kgs. Lyngby, Denmark

⁴SUPA, School of Physics and Astronomy, University of St. Andrews, Scotland, United Kingdom

⁵Institut de Physique, Ecole Polytechnique Fédérale de Lausanne, 1015 Lausanne, Switzerland

(Dated: July 13, 2021)

Among all transition metals, Palladium (Pd) has the highest density of states at the Fermi energy yet does not fulfill the Stoner criterion for ferromagnetism. However, its close vicinity to magnetism renders it a nearly ferromagnetic metal, which hosts paramagnons, strongly damped spin fluctuations. In this letter we compare the total and the differential conductance of mono-atomic Pd and Cobalt (Co) contacts between Pd electrodes. Transport measurements reveal a conductance for Co of $1 G_0$, while for Pd we obtain $2 G_0$. The differential conductance of mono-atomic Pd contacts shows a drop with increasing bias, which gives rise to a peculiar Λ -shaped spectrum. Supported by theoretical calculations we correlate this finding with the life time of hot quasi-particles in Pd which is strongly influenced by paramagnon scattering. In contrast to this, Co adatoms locally induce magnetic order and transport through single cobalt atoms remains unaffected by paramagnon scattering, consistent with theory.

PACS numbers: 72.15Qm, 68.37.Ef

Spin fluctuations are believed to provide the pairing glue in unconventional superconductors [1–4]. Therefore, the interaction of magnetic fluctuations with electronic degrees of freedom is critical for a full understanding of unconventional superconductivity. A material which in its elemental form exhibits strong magnetic fluctuations yet does not even become a conventional superconductor is palladium [5]. This raises important questions as to how spin fluctuations interact with the conduction band electrons.

Spin fluctuations also play an important role in some of the macroscopic properties of elemental metals: Both, palladium (Pd) and platinum (Pt) are not ferromagnetic despite an only partially filled d -shell, but belong to a class of materials coined *nearly* ferromagnetic metals [6]. Pd possesses the highest density of states (DOS) at the Fermi energy (E_F) among all transition metals and the Stoner criterion is almost fulfilled [7] bringing it right to the edge to ferromagnetism. In these nearly ferromagnetic metals, strongly damped spin fluctuations, known as paramagnons, have a great impact on macroscopic quantities such as the heat capacity and magnetic susceptibility [8]. Paramagnons in Palladium have been commonly observed by means of scattering techniques such as neutron scattering [9] and angle-resolved photoemission [10] within an energy range of about 50-150 meV - detection on the atomic level, however, remained illusive.

Paramagnons can be described as magnetic fluctuations of a paramagnetic phase [11]. In contrast to magnons, which are the fluctuations of a magnetically ordered system, paramagnons are collective overdamped modes with only short correlation lengths that appear close to a magnetic instability [6, 12]. Recent experimental [7, 13–16] and theoretical [17–22] studies have explored the possibility of Pd becoming ferromagnetic in nanostructures. In this work we study trans-

port through single Pd and Co adatoms on a Pd(111) surface by scanning tunneling microscopy (STM). Differential conductance (dI/dV) spectra were taken at different tip-sample distances z from the tunneling to the contact regime. In Pd contacts, we find that the spectral features show a significant decrease of the conductance with increasing bias, independent of the polarity. Theoretical calculations show that this feature can be correlated to the extremely short lifetime of hot quasi-particles in Pd – an effect that we attribute to paramagnon excitations. For Co contacts, the differential conductance is comparatively featureless.

Experiments have been performed on a Pd(111) single crystal with a home-built UHV-STM operating at 6 K. The sample was cleaned in vacuum with a base pressure of $3 \cdot 10^{-10}$ mbar by numerous cycles of Ar⁺ sputtering and subsequent annealing. The most frequent bulk contaminants in Pd are sulphur (S) and carbon (C). Upon annealing to temperatures of 1000 K for extended periods, S and C impurities migrate to the surface. S is removed by sputtering, while C is removed by exposing the crystal to an oxygen atmosphere ($p_{O_2} = 3.0 \cdot 10^{-7}$ mbar) for 20 min while heating the sample to temperatures in the range of 650-850 K. The final preparation cycle was carried out in the absence of oxygen and the sample was annealed to 900 K. The apex of the STM tip was covered with Pd by gentle indentation into the surface. Single Pd atoms were released from the tip by approaching the tip towards the bare surface until contact is formed [Fig. 1(a)]. Co atoms were evaporated from a wire with 99.99% purity in-situ onto the sample being held at 6 K [Fig. 1(b)]. Both species can be easily distinguished from each other by their apparent height [Fig. 1(c),(d),(e)]

Distance dependent conductance, $G(z)$, measurements have been carried out for contacts between the tip and in-

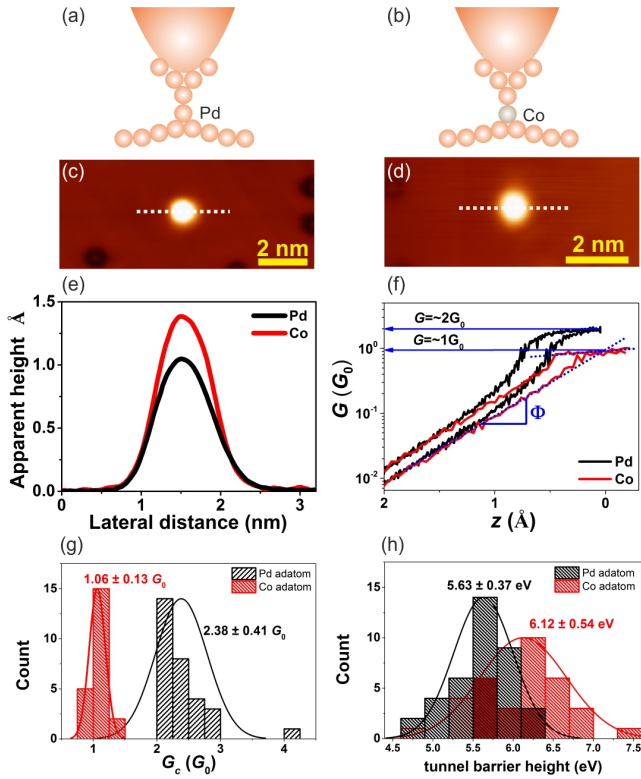


Figure 1. (a),(b) Sketch of mono-atomic Pd (a) and Co (b) contacts. (c),(d) Constant current images of a Pd (c) and a Co (d) adatom acquired on Pd(111) at 6 K ($V = 0.1\text{V}$, $I = 100\text{pA}$). (e) Apparent height profile of a single Pd and Co atom. f, Conductance-displacement ($G(z)$) curves taken on Pd (solid black line) and Co (solid red line). Mono-atomic Pd contacts show a characteristic conductance of about $2G_0$ while Co contacts exhibit ones of about $1G_0$. (g),(h) Conductance and tunnel barrier height measurements on Pd and Co adatoms deposited onto Pd(111). To extract the mean values, the histograms were fitted with Gaussian functions.

dividual Pd and Co adatoms. From the $G(z)$ curves two regimes are discernible; a tunneling and a contact regime [Fig. 1(f)]. In the tunneling regime, a decrease in z is associated with an exponential increase of the conductance, i. e. $G(z) = G_0 \exp(-2\kappa z)$ (with $G_0 = 2e^2/h = 77.5\mu\text{S}$ as the quantum of conductance). The slope $\kappa = \sqrt{\frac{m_0}{\hbar^2} \Phi}$ is directly related to the local tunnel barrier height Φ [23]. Reducing z further leads to a relaxation of the tip and the surface atoms due to adhesive forces. When contact between the tip apex atom and the surface is established, a discontinuous jump in $G(z)$ occurs. This jump arises when the bonding strength between surface and tip apex atom overcomes that between the atoms within the tip. As displayed in Fig. 1(f) for the approach curve on a Co atom, the conductance of the contact G_c can be obtained by extrapolating the tunneling regime to the intersection with the contact regime, which is defined as $z = 0$. Positive z values denote tunneling, whereas negative ones the contact regime.

The measured values of G_c and Φ for both types of adatoms are summarized in Fig. 1(g) and (h). For the tip-Pd adatom and tip-Co adatom contacts we found $G_c = 2.38 \pm 0.41 G_0$

and $1.06 \pm 0.13 G_0$, respectively. The results for Co adatoms are consistent with previous reports for Co adatoms on noble metal surfaces [24, 25]. For Pd contacts, the reported values exhibit variations depending on preparation conditions. For break junctions prepared in vacuum at room temperature, a conductance of $0.5G_0$ was found and interpreted in terms of a single spin-polarized conductance channel [15]. Other measurements carried out on Pd break junctions at low temperatures and in vacuum reported conductances in good agreement with our values[26, 27].

Differential conductance (dI/dV) spectra were obtained on top of Pd and Co adatoms starting from the tunneling regime to contact [Fig. 2(a),(b)]. Spectra taken on the Pd adatoms in the tunneling regime give access to the distribution of occupied and unoccupied states near E_F , hence reflecting the LDOS of Pd [8]. However, when the contact regime is reached a drastic change of the feature to a distinct Λ -shaped peak occurs. Further increasing the setpoint G leads to a significant broadening and decrease of the signal strength of the Λ -like feature. Contrary to these observations the dI/dV spectra taken on Co adatoms show a rather flat signal in the tunneling as well as in the contact regime. The small feature on the cobalt atoms around zero bias might be due to emergent Kondo correlations, which are commonly observed for magnetic adatoms on noble metal surfaces [28, 29].

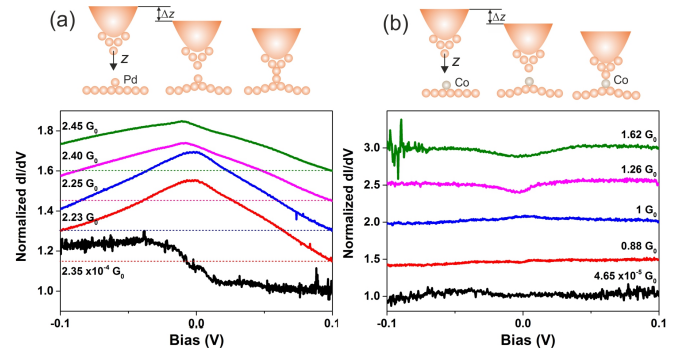


Figure 2. Differential conductance (dI/dV) acquired on a Pd adatom (a) and Co adatom (b) deposited on Pd(111). Spectra were recorded with a lock-in modulation of 2mV and taken through different heights from tunneling to contact as indicated by the setpoint conductance. Curves are normalized at $V = 0.1\text{V}$ (horizontal dashed lines) and stacked for clarity.

To understand the Λ anomaly, we have performed Density Functional Theory (DFT) and electronic transmission calculations in the Non Equilibrium Green Function (NEGF) formalism with the Atomistix Toolkit (ATK) code from QuantumWise[30] and the Transiesta code[31] to model the transport through single cobalt and palladium adatoms. All our calculations were performed within the local density approximation (LDA) using the Perdew Zunger parametrization [32] since the generalized gradient approximation incorrectly predicts a magnetic ground state for Pd [33][34]. We used

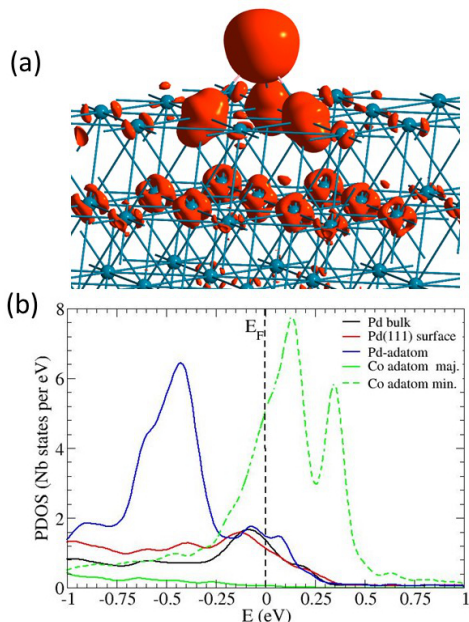


Figure 3. (a) Real-space distribution of the spin-density isosurface plot of a Co adatom on a Pd(111) surface. The magnetic moment on the cobalt atom is $2.76\mu_B$, while the one induced on the palladium atoms is $0.26\mu_B$ on the nearest neighbours and $0.13\mu_B$ in the sub-layer. (b) Calculated projected density of states (PDOS) on the d orbitals of a bulk (black), (111) surface atom (red), Pd (blue) and Co (green) adatom. In the case of the Cobalt adatom the majority spin (full green) and the minority spin (dashed green) are splitted by a large exchange and the principal PDOS contribution from the majority spin is well below $E_F - 1\text{eV}$ while for palladium there is no magnetism and the two spins are degenerate.

a single zeta polarized (SZP) basis set and separable norm-conserving Troullier-Martins pseudopotentials[35] with partial core corrections.

We have performed DFT calculations for these two systems to establish the differences in the electronic states near E_F . We found no evidence of spin-polarization for the Pd adatom, while a strong spin polarization develops on the Co adatom with a spin moment of $2.76\mu_B$. In addition, we find non-negligible spin-polarization on neighboring Pd atoms, indicating that the Co atom locally induces magnetic order [Fig. 3(a)].

Fig. 3(b) depicts the projected density of states (PDOS) of the d orbitals for a bulk and surface Pd atom as well as for the adatom (Pd or Co). The d band of Pd is almost filled and E_F falls into the tail of the d -states[36]. For Cobalt, the d -states exhibit a strong exchange splitting. The states at E_F are dominated by d -states of minority spin character.

A series of electronic transport calculations was carried out where the system is divided into three regions: left and right leads and central region containing the atomic contact. The leads are built from a semi-infinite repetition of 3 atomic layers with an fcc stacking. A 4×4 unit cell is used and periodic boundary conditions are applied in the (111) plane. We

checked that a 5×5 unit cell did not change our results significantly. The central part is made of 3 layers in contact via a 4 atom pyramid the apex of which is at a distance d from the adatom. Only the adatom and the pyramid have been allowed to relax. A sketch of the system is presented in the inset of Fig. 4(a).

The electronic transmission through a Pd adatom as a function of the energy [Fig. 4(a)] depends crucially on the tip-adatom distance d but for distances between 3 \AA and 2.6 \AA the typical conductances are on the order of $(2-2.5) G_0$, which is in the range of the experimental values. It is also of the same order of magnitude as found by Gava *et al.* [22] for the transmission between two Pd(001) surfaces connected by a small atomic chain.

The transmission through a magnetic Co adatom drops drastically (by a factor of two) compared to the case of the Pd adatom. For the sake of comparison we have calculated the transmission through a hypothetical non-magnetic Co adatom for which the conductance at E_F is close to the one of the Pd adatom confirming the influence of the local magnetization on the electronic transmission. These theoretical results are perfectly consistent with the experimental ones.

The complete modeling of the differential conductance curves is rather cumbersome since this would involve the calculation of the electrical current at various bias voltages and then calculating the derivative of $I(V)$. However in the present case, in the contact regime, for a highly symmetric system (identical leads) and in a very narrow voltage range around the Fermi level, one expects an almost odd $I(V)$ curve and therefore an even dI/dV curve which can safely be approximated by the average transmission, $\frac{1}{2}[T(E = -\frac{V}{2}) + T(E = \frac{V}{2})]$. Using this approximation we find flat and featureless dI/dV spectra for bias voltages between -0.1 and 0.1 V at tip-adatom distances between 2.5 and 3 \AA for both, Co and Pd contact, which do not reproduce the experimental findings.

The discrepancy between the experimentally observed and calculated conductance spectra can be lifted when taking the finite lifetime of the hot quasiparticles into account. The quasiparticle lifetime in Pd has been calculated using various GW-based many-body perturbation theories[37, 38] showing considerably shorter lifetimes close to E_F compared to, e. g., Au or Cu. It is also displaying a different behavior compared to the free-electron behavior in Fermi liquid theory, $\hbar/\tau = \Gamma \propto (E - E_F)^2$. This is attributed to the role of the d -electrons and their finite bandwidth. Early calculations[39] using a finite bandwidth model for an almost full band suggested an electronic level broadening due to spin-fluctuations in Pd of $\Gamma(E) \approx 0.05|E - E_F|$. Lifetimes τ calculated within the GW approximation[38] result in $\tau \sim 10 \text{ fs}$ corresponding to $\Gamma \approx 50 \text{ meV}$ for $E - E_F \approx 250 \text{ meV}$. Based on this we add an additional bias-dependent contribution to the imaginary part of the self-energy, $\Gamma(V) = \alpha|eV|$, to the d -orbitals

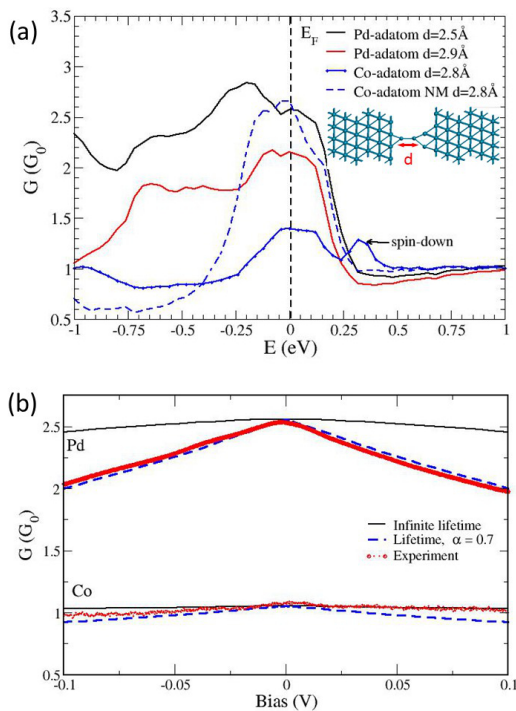


Figure 4. (a) Calculated electronic transmission between a tip and a monatomic Pd (Co) adatom. d is the distance between the adatom and the apex of the tip. In the case of the Co adatom the system is spin polarized. Additionally we have also considered the case of a non-magnetic (NM) Co adatom. The sharp feature above 0.25 eV (indicated by an arrow) originates from the spin-down contribution. The Fermi level is set as the zero of energy. (b) Differential conductance (dI/dV) calculated with and without including a lifetime broadening, $\Gamma(V) = \alpha|V|$, in the electrodes. The parameter α is fitted to the experimental results.

in the two outermost surface layers in the calculation. This corresponds to the lifetime of electrons injected from the negative electrode that enter eV above the Fermi level in the positive electrode. If we fit the unknown α to the experiments, as shown in Fig. 2(d), we obtain $\alpha \sim 0.7$ corresponding to a lifetime of roughly 10 fs at a bias of 100 mV slightly below the GW results.

It is interesting to note that similar spectroscopic features have been observed in mesoscopic contacts with conductances on the order of about $100 G_0$ and $800 G_0$, respectively [16, 26]. While the details might differ, we expect that the mechanism leading to the suppression of conductance with increasing bias voltage in those contacts is the same.

Based on the theoretical calculations we attribute the decrease of the conductance with increasing bias to a suppression of the transmission of electrons. With increasing energy, more paramagnons are excited and more charge carriers are reflected. A characteristic feature of paramagnons is that they are overdamped modes, meaning they have short lifetimes and couple strongly to electrons to release their energy. As a consequence, their response in momentum space is broad and not distinctly defined giving rise to a broad and smeared out fea-

ture similar to what we observe. The strongest argument for the presence of paramagnons in Palladium is the extremely short lifetime of quasiparticles that is obtained from the fit to the observed spectra. The different slopes of the dI/dV spectra for Pd and Co contacts depicted in Fig. 4(b) are directly related to the magnetism of the Co adatom. While for palladium, the d -states at the Fermi level contribute substantially to the conductance, for cobalt the exchange coupling pushes the majority- d -states below the Fermi level, and thus it is only spin-majority states of s -character and spin-minority states of d -character which contribute to the transport. The electronic states of s -character are only weakly affected by paramagnetic excitations, and therefore the Λ -shape is suppressed.

In conclusion, we have studied atomic contacts consisting of single Pd and Co atoms. Contacts of single Pd atoms exhibit pronounced Λ -shaped spectra, which we attribute to strong electron scattering near the contact which limits the lifetime of the charge carriers. This effect is explained by the presence of paramagnons. Conversely, contacts consisting of Co adatoms, which locally induce magnetic order, do not exhibit a similar suppression of conductance. Hence, we have demonstrated that signatures of paramagnons, which were commonly investigated by means of scattering techniques that integrate over larger areas, can be detected with local probes. This might expand the experimental tools for the investigation of high-temperatures superconductors.

ACKNOWLEDGEMENT

VS, US, BB acknowledge funding by the SFB 767 and the Emmy-Noether-Program of the Deutsche Forschungsgemeinschaft. CB and MB would like to thank Derek Stewart for providing the pseudo-potential of palladium.

* Corresponding author; electronic address: verena.schendel@kit.edu

- [1] D. Fay and J. Appel, Phys. Rev. B **22**, 3173 (1980).
- [2] T. Moriya, Y. Takahashi, and K. Ueda, Journal of the Physical Society of Japan **59**, 2905 (1990).
- [3] N. D. Mathur, F. M. Grosche, S. R. Julian, I. R. Walker, D. M. Freye, R. K. W. Haselwimmer, and G. G. Lonzarich, Nature **394**, 39 (1998).
- [4] D. J. Scalapino, Rev. Mod. Phys. **84**, 1383 (2012).
- [5] B. Stritzker, Phys. Rev. Lett. **42**, 1769 (1979).
- [6] G. G. Lonzarich and L. Taillefer, Journal of Physics C: Solid State Physics **18**, 4339 (1985).
- [7] D. A. van Leeuwen, J. M. van Ruitenbeek, G. Schmid, and L. de Jongh, Physics Letters A **170**, 325 (1992).
- [8] F. M. Mueller, A. J. Freeman, J. O. Dimmock, and A. M. Furdyna, Phys. Rev. B **1**, 4617 (1970).
- [9] R. Double, S. M. Hayden, P. Dai, H. a. Mook, J. R. Thompson, and C. D. Frost, Phys. Rev. Lett. **105**, 027207 (2010).
- [10] H. Hayashi, K. Shimada, J. Jiang, H. Iwasawa, Y. Aiura, T. Oguchi, H. Namatame, and M. Taniguchi, Phys. Rev. B **87**, 035140 (2013).

- [11] O. P. Sushkov, *Nature Physics* **10**, 339 (2014).
- [12] T. Moriya and Y. Takahashi, *Le Journal de Physique Colloques* **39**, C6 (1978).
- [13] X. Teng, W. Q. Han, W. Ku, and M. Hückler, *Angewandte Chemie - International Edition* **47**, 2055 (2008).
- [14] C. Xiao, H. Ding, C. Shen, T. Yang, C. Hui, and H. J. Gao, *Journal of Physical Chemistry C* **113**, 13466 (2009).
- [15] V. Rodrigues, J. Bettini, P. C. Silva, and D. Ugarte, *Phys. Rev. Lett.* **91**, 096801 (2003), arXiv:0307284 [cond-mat].
- [16] K. Ienaga, H. Takata, Y. Onishi, Y. Inagaki, H. Tsujii, T. Kimura, T. Kawae, K. Ienaga, H. Takata, Y. Onishi, Y. Inagaki, H. Tsujii, T. Kimura, and T. Kawae, *Applied Physics Letters* **106**, 2 (2015).
- [17] K. Lee, *Phys. Rev. B* **58**, 2391 (1998).
- [18] A. Delin, E. Tosatti, and R. Weht, *Phys. Rev. Lett.* **92**, 057201 (2003).
- [19] K. M. Smelova, D. I. Bazhanov, V. S. Stepanyuk, W. Hergert, A. M. Saletsky, and P. Bruno, *Phys. Rev. B* **77**, 033408 (2008).
- [20] Y. B. Kudasov and A. S. Korshunov, *Physics Letters, Section A: General, Atomic and Solid State Physics* **364**, 348 (2007).
- [21] Y. Sun, J. D. Burton, and E. Y. Tsybal, *Phys. Rev. B* **81**, 064413 (2010).
- [22] P. Gava, A. Dal Corso, A. Smogunov, and E. Tosatti, *European Physical Journal B* **75**, 57 (2010).
- [23] G. Binnig, H. Rohrer, C. Gerber, and E. Weibel, *Applied Physics Letters* **40**, 178 (1982).
- [24] N. Néel, J. Kröger, L. Limot, K. Palotas, W. A. Hofer, and R. Berndt, *Phys. Rev. Lett.* **98**, 016801 (2007).
- [25] L. Vitali, R. Ohmann, S. Stepanow, P. Gambardella, K. Tao, R. Huang, V. S. Stepanyuk, P. Bruno, and K. Kern, *Phys. Rev. Lett.* **101**, 216802 (2008).
- [26] S. Csonka, A. Halbritter, G. Mihály, O. I. Shklyarevskii, S. Speller, and H. Van Kempen, *Phys. Rev. Lett.* **93**, 016802 (2004).
- [27] T. Matsuda and T. Kizuka, *Japanese Journal of Applied Physics*, **46**, 4370 (2007).
- [28] M. Ternes, A. J. Heinrich, and W.-D. Schneider, *J. Phys.: Condens. Matter* **21**, 053001 (2009).
- [29] M. Schneider, L. Vitali, P. Wahl, N. Knorr, L. Diekhoner, G. Wittich, M. Vogelgesang, and K. Kern, *Applied Physics A* **80**, 937 (2005).
- [30] Atomistix ToolKit version 2015.1, QuantumWise A/S (www.quantumwise.com).
- [31] M. Brandbyge, J.-L. Mozos, P. Ordejón, J. Taylor, and K. Stokbro, *Phys. Rev. B* **65**, 165401 (2002).
- [32] J. P. Perdew, *Phys. Rev. B* **23**, 5048 (1981).
- [33] S. S. Alexandre, M. Mattesini, J. M. Soler, and F. Yndurain, *Phys. Rev. Lett.* **96**, 079701; author reply 079702 (2006).
- [34] Our LDA calculations predict an equilibrium lattice parameter of 3.87 Å for face centered (fcc) Pd and an on-set of magnetism for lattice parameters above 3.96 Å while GGA calculations predict a magnetic bulk at equilibrium.
- [35] N. Troullier and J. L. Martins, *Phys. Rev. B* **43**, 1993 (1991).
- [36] Note that when considering the effect of a tip in contact with the adatom we have found that a rather pronounced dip develops around E_F which will play strongly against the magnetization of the adatom.
- [37] F. Ladstädter, U. Hohenester, P. Puschnig, and C. Ambrosch-Draxl, *Phys. Rev. B* **70**, 235125 (2004).
- [38] V. P. Zhukov, E. V. Chulkov, and P. M. Echenique, *Phys. Rev. B* **72**, 155109 (2005).
- [39] J. P. Longo and B. Mitrović, *J. Low Temp. Phys.* **74**, 141 (1989).